

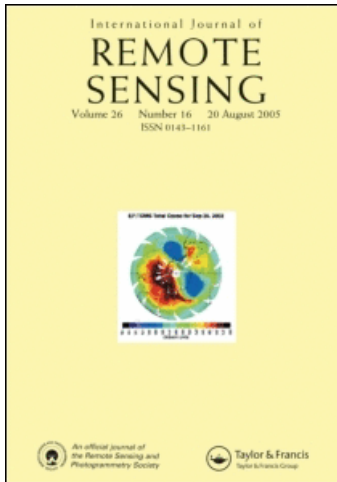
This article was downloaded by: [Stewart, S. F.]

On: 31 October 2008

Access details: Access Details: [subscription number 904869229]

Publisher Taylor & Francis

Informa Ltd Registered in England and Wales Registered Number: 1072954 Registered office: Mortimer House, 37-41 Mortimer Street, London W1T 3JH, UK



International Journal of Remote Sensing

Publication details, including instructions for authors and subscription information:

<http://www.informaworld.com/smpp/title-content=t713722504>

Monitoring active subglacial volcanoes: a case study using airborne remotely sensed imagery of Grímsvötn, Iceland

S. F. Stewart ^a; H. Pinkerton ^a; G. A. Blackburn ^b; M. T. Gudmundsson ^c

^a Department of Environmental Science, Lancaster University, Lancaster LA1 4YB, UK ^b Department of Geography, Lancaster University, Lancaster LA1 4YB, UK ^c Institute of Earth Sciences, University of Iceland, 101 Reykjavik, Iceland

Online Publication Date: 01 November 2008

To cite this Article Stewart, S. F., Pinkerton, H., Blackburn, G. A. and Gudmundsson, M. T. (2008) 'Monitoring active subglacial volcanoes: a case study using airborne remotely sensed imagery of Grímsvötn, Iceland', *International Journal of Remote Sensing*, 29:22,6501 — 6514

To link to this Article: DOI: 10.1080/01431160802168186

URL: <http://dx.doi.org/10.1080/01431160802168186>

PLEASE SCROLL DOWN FOR ARTICLE

Full terms and conditions of use: <http://www.informaworld.com/terms-and-conditions-of-access.pdf>

This article may be used for research, teaching and private study purposes. Any substantial or systematic reproduction, re-distribution, re-selling, loan or sub-licensing, systematic supply or distribution in any form to anyone is expressly forbidden.

The publisher does not give any warranty express or implied or make any representation that the contents will be complete or accurate or up to date. The accuracy of any instructions, formulae and drug doses should be independently verified with primary sources. The publisher shall not be liable for any loss, actions, claims, proceedings, demand or costs or damages whatsoever or howsoever caused arising directly or indirectly in connection with or arising out of the use of this material.

Monitoring active subglacial volcanoes: a case study using airborne remotely sensed imagery of Grímsvötn, Iceland

S. F. STEWART*†, H. PINKERTON†, G. A. BLACKBURN‡ and
M. T. GUDMUNDSSON§

†Department of Environmental Science, Lancaster University, Lancaster LA1 4YB, UK

‡Department of Geography, Lancaster University, Lancaster LA1 4YB, UK

§Institute of Earth Sciences, University of Iceland, Sturlugata 7, 101 Reykjavík, Iceland

Grímsvötn is located beneath Vatnajökull, Europe's largest temperate ice cap. As a part of ongoing research on heat flux, morphological changes and volcanic processes at Grímsvötn, Airborne Thematic Mapper (ATM) imagery and aerial photographs were acquired in 2001. The thermal images illuminated distinct areas of geothermal activity along the southern caldera wall. In combination with meteorological data the images were used to estimate surface temperatures and heat flux from patches of open water along the margin of the ice shelf covering the Grímsvötn subglacial lake. It was found that water temperatures varied from 0°C to ~45°C and that the heat flux to the atmosphere from open water varied from slightly negative values (net energy gain) up to 1000 W m⁻². The total heat output from the ~0.1 km² of open water was estimated as ~18 MW, about 1% of the base heat output of Grímsvötn. The aerial photographs were used to produce geomorphological maps of the caldera wall, including areas that cannot be safely mapped from the ground. This work indicates that thermal imagery can be an important supplement to ground-based measurements, and that combined optical and thermal remote sensing is a useful tool for spatially detailed monitoring of inaccessible and partly ice-covered volcanoes.

1. Introduction

Traditional field-based methods for monitoring active volcanoes are difficult to use on ice-covered volcanoes because of problems with access and hazards associated with rapid melting of ice and snow during an eruption. Temperate glaciers, such as those in Iceland, are at their pressure melting temperature throughout their thickness and water can migrate beneath the glacier, allowing meltwater to flow from a geothermal heat source to the edges of the glacier causing devastating jökulhlaups (Smellie 1999), such as the 1996 Gjálp jökulhlaup in Iceland (Björnsson 2003). Consequently, an improved understanding of processes and alternative methodologies for monitoring subglacial volcanoes, and improving hazard mitigation, would be useful.

Grímsvötn is Iceland's most active volcano (e.g. Gudmundsson 1989, Thordarson and Larsen 2007) and is relatively inaccessible and hazardous, being located within Vatnajökull, Europe's largest temperate ice sheet (figure 1). Mapping of subglacial topography using radio echo sounding has shown that Grímsvötn has a composite caldera, made up of three smaller calderas: main (or south), north and east calderas (Björnsson 1988, Gudmundsson 1989). The 20 km²

*Corresponding author. Email: kina.stewart@lebp.co.uk

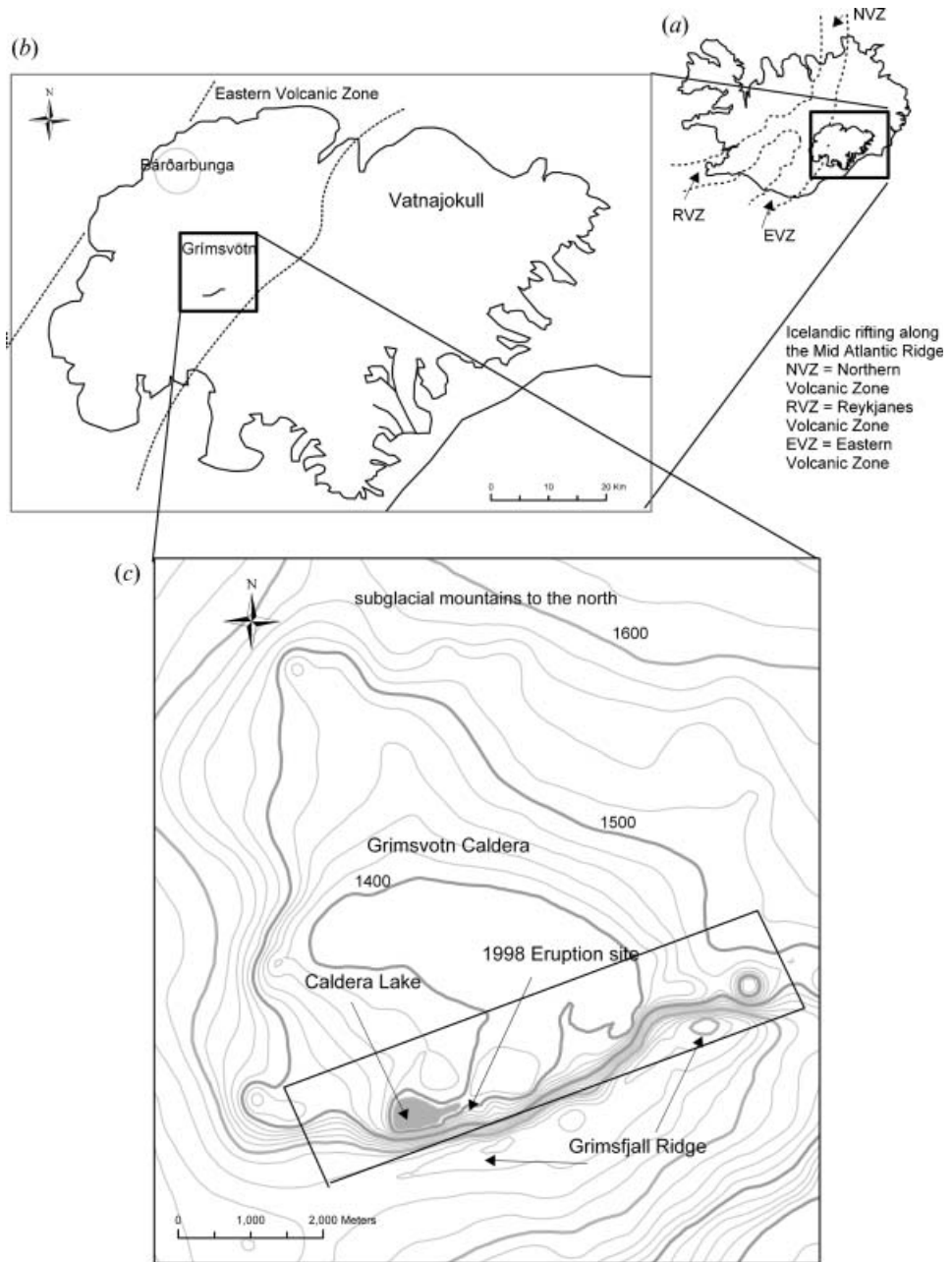


Figure 1. (a) A map of Iceland with the volcanic zones and location of Vatnajökull ice sheet, (b) the location of Grímsvötn in relation to the Vatnajökull ice sheet, and (c) a contour map of the Grímsvötn caldera created in 2001 by Icelandic collaborators, using differential GPS. The Grímsfjall ridge, crater lake, and the 1998 eruption site are labelled. The rectangular box over the Grímsfjall ridge shows the land area covered by the aerial survey.

main caldera is the largest and has been the focus of recent geothermal and volcanic activity. The northern slope of the Grímsfjall ridge marks the southern wall of the main caldera, the only part of the volcano where rock is exposed.

Within the Grímsvötn caldera, intense geothermal activity continuously melts the surrounding ice above at a rate of $0.2\text{--}0.5\text{ km}^3\text{ year}^{-1}$ (Björnsson and Gudmundsson 1993, Björnsson 2003), creating permanent depressions or ice cauldrons above the activity. Due to the high ice overburden pressure, meltwater is trapped as a subglacial lake. Above the caldera lake a floating 250-m-thick ice shelf is found. Meltwater accumulates in the subglacial caldera lake, causing increases of $\sim 10\text{--}30\text{ m year}^{-1}$ of the floating ice. The meltwater is subsequently released in jökulhlaups when the seal surrounding the lake is breached, causing the lake level to lower by 50–130 m within 1–2 weeks, releasing $2\text{--}5\text{ km}^3$ of water every 4 to 6 years (Björnsson and Gudmundsson 1993). The area and volume of the subglacial lake has varied over time. Over the seven decades of observation, decreased geothermal activity has led to shrinking of the lake; Gudmundsson *et al.* (1995) showed that the area of the lake at its maximum extent prior to jökulhlaups changed from $30\text{--}37\text{ km}^2$ in 1930–1960 to $15\text{--}20\text{ km}^2$ after 1980. It is argued that these meltwater outbursts can trigger small volcanic eruptions due to pressure release, as in the 1934 and 2004 eruptions (Einarsson *et al.* 1997, Smithsonian Institution 2004). The high geothermal heat allows for areas of open water to be present at times. Consequently, exposed lakes can be found above particularly intense geothermal activity (Gudmundsson 1989).

Björnsson (1983) showed that Grímsvötn could be used as a calorimeter to estimate heat flow from a geothermal area. At that time, an ice sheet covered and insulated the thermal area, stopping heat from escaping to the atmosphere. Therefore, any ice melted at the base is a measure of the heat released by thermal activity at the glacier base (Gudmundsson 2003). The heat output has been mostly in the range of 1500–4000 MW over the past several decades (Björnsson 1983, Björnsson and Gudmundsson 1993).

The present study complements and extends the multidisciplinary work currently used to monitor Grímsvötn (Gudmundsson *et al.* 2004, Sigmundsson and Gudmundsson 2004, Vogfjörd *et al.* 2005). The aim of this work was to establish the usefulness of remotely sensed data for providing contributions to two inter-related research foci: heat flux estimates and geomorphological mapping.

2. Background

2.1 Heat flux estimates

Observations that can be used to study variations in the thermal output of the Grímsvötn caldera have been made since 1934, allowing the ice-covered Grímsvötn caldera lake to be used as a calorimeter to measure the heat transfer from magma to ice and meltwater (Björnsson and Gudmundsson 1993, Gudmundsson *et al.* 1995). However, this work was carried out on the Grímsvötn caldera lake prior to the 1996 Gjálp eruption, when the lake was considered to be an enclosed system with no leakage. Since the 1996 eruption, increased melting at the ice dam that sealed Grímsvötn caldera lake has led to leakage from the lake (Björnsson 2003). Consequently, calorimetry based only on water accumulation within the lake can no longer be used effectively. However, temperatures recorded from crater lakes and other spots where the subglacial lake is exposed are potentially very useful for monitoring Grímsvötn.

The present study investigated the potential for using remotely sensed thermal imagery along with ground-based meteorological measurements to calculate heat

flux to the atmosphere from the 1998 eruption crater lake and other spots of open water. This component of the heat budget of Grímsvötn has not been studied before, but when parts of the caldera lake are not covered by an ice shelf this may provide a substantial part of the overall heat flux.

2.2 Geomorphological mapping

Grímsvötn contains a range of geomorphological features formed by a number of processes, including ash falls, avalanches and jökulhlaups (Björnsson 2004). Moreover, morphological features are present, such as crevasses and ice caves, that are potentially useful for monitoring changes in volcanic or subvolcanic processes. Aerial photographs obtained during the 2001 overflight of Grímsvötn were used to construct a geomorphological map of the Grímsfjall Ridge area of Grímsvötn.

3. Methodology

In 2001, the Natural Environment Research Council (NERC) Airborne Research and Survey Facility (ARSF) carried out an aerial survey of Grímsvötn. Multispectral imagery was acquired by an Airborne Thematic Mapper (ATM) sensor and aerial photographs from a Wild RC-10 camera covering the Grímsfjall Ridge section of the caldera on 10 and 14 June. An expedition visiting Grímsvötn on 2–9 June inspected the crater lake and its surroundings. No soundings of water temperature could be made because of the steep and unstable banks but photographs were taken that aid in the interpretation of the thermal imagery.

3.1 Heat flux estimates

The ATM thermal imagery (figure 2) was preprocessed using a temperature conversion program devised by A. Wilson (personal communication, 2003). The algorithm included a correction for sensor response and wavelength (Stewart *et al.* 2007). The conversion assumed that the ground surface acts as a blackbody. Consequently, an emissivity of 1 was used in Planck's law to calculate temperature. The following equation is a variation of Planck's formula, with the added sensor response from the Wilson (2003) program:

$$M_{\lambda} = \frac{C_1 \lambda^{-5} \text{resp}}{\exp(C_2/\lambda T) - 1} \quad (1)$$

where M_{λ} is the radiant exitance, C_1 ($=119095879.96 \text{ W m}^2$) and C_2 ($=14387.75225 \text{ W m}^2$) are spectral radiance constants, resp=sensor response, λ =wavelength (μm) and T =temperature (K).

Using Wilson's program, the spectral radiance curve was separated into 141 wavelength divisions based on the sensor response. Temperature was iterated until the radiance matched the radiance from the image for a given pixel. This process was continued for every pixel in the image until all pixels had a temperature assigned within a new array (Stewart *et al.* 2007).

Figure 3 is a temperature frequency distribution curve of the 1998 crater lake (see figure 2) derived from the ATM images acquired on 10 and 14 June 2001. This shows that the overall distribution of temperatures is similar for the two dates. For the calculation of heat flux, a mean temperature for the whole lake for each date was taken from the distribution in figure 3.

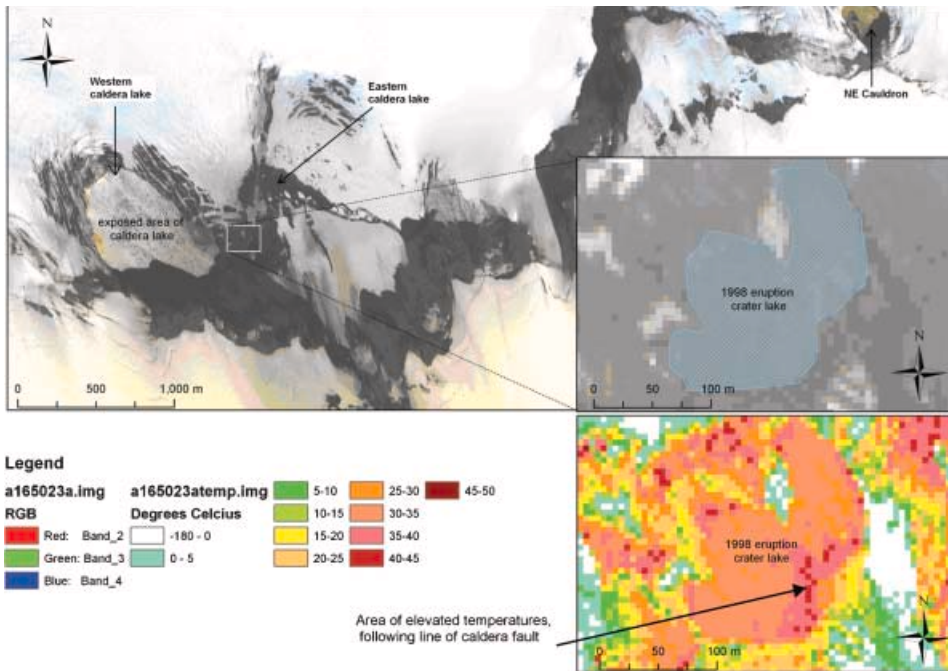


Figure 2. Colour composite ATM image (ATM bands 2, 3, 4), with the 1998 crater lake inset, and a temperature image of the 1998 eruption crater lake from which the temperatures were taken to calculate heat flux. Western and eastern caldera lakes, the northeast cauldron and the 1998 eruption crater lake are shown.

Meteorological data covering the times of the aerial surveys were acquired from the Grímsvötn weather station and the Skaftafell station, 50 km south of Grímsvötn. Skaftafell is at a lower altitude than the study site and not on the ice sheet, but was the closest station with measurements of meteorological variables that were not recorded at Grímsvötn. The relative humidity data necessary for the calculations came from an average of two other nearby meteorological weather stations, Akurnes and Kirkjubaejarklaustur, neither of which are located on the ice sheet.

The total upward heat flux (Q_T) from the Grímsvötn lake is the sum of all the fluxes from individual processes (Gill 1982, Jones *et al.* 2005), namely,

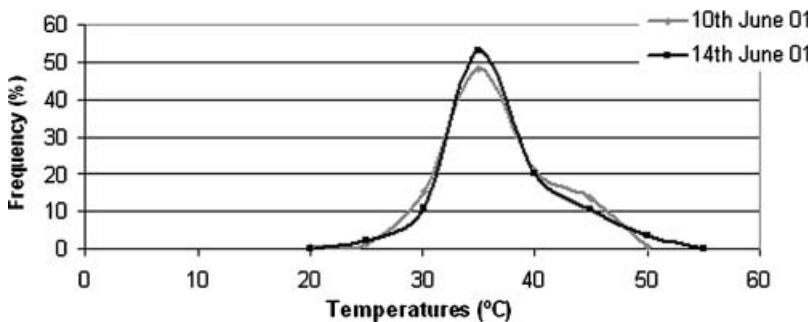


Figure 3. Histogram of temperatures within the Grímsvötn 1998 crater lake for 10 and 14 June 2001.

$$Q_T = Q_{Lo} + Q_{Sh} + Q_{LE} - Q_{Si} \quad (2)$$

where Q_{Lo} is the net upward longwave radiation, Q_{Sh} is the sensible heat flux, Q_{LE} is the latent heat flux and Q_{Si} is the incoming shortwave solar radiation. Each parameter was derived from the following equations.

$$Q_{Lo} = \varepsilon_s \sigma T_s^4 \quad (3)$$

$$Q_{Sh} = \rho C_p C_e U_a (T_s - T_a) \quad (4)$$

$$Q_{LE} = \rho C_e L U_a (q^*_s - q_a) \quad (5)$$

As specific heat capacity, density of air and latent heat of evaporation undergo only small changes with temperature (Jones *et al.* 2005), constant values have been assigned from the literature. The emissivity of water, ε_s , is 0.985, σ is the Stefan–Boltzmann constant $5.67 \times 10^{-8} \text{ W m}^{-2} \text{ K}^{-4}$ (Oke 1995), air density, ρ , is 1 kg m^{-3} (Garratt 1992), the specific heat capacity of air, C_p , is $1005 \text{ J kg}^{-1} \text{ K}^{-1}$ (Gill 1982, Garratt 1992), the transfer coefficient for sensible and latent heat, C_e , is 1.4×10^{-3} (Hicks 1972, Jones *et al.* 2005), U_a is wind speed in m s^{-1} , L is latent heat of evaporation $2.5 \times 10^6 \text{ J kg}^{-1}$ (Gill 1982, Garratt 1992). T_s is the lake surface temperature in K, T_a is mean air temperature in K, the saturated specific humidity at the water surface is q^*_s , and the specific humidity at the reference height (10 m above lake surface) is q_a .

To calculate the outgoing longwave radiation, Q_{Lo} , a correction for cloud cover and back radiation is added to the basic equation. For example,

$$Q_{Lo} = \varepsilon_s \sigma T_s^4 (0.39 - 0.05 e_a^{1/2}) (1 - 0.6 n_c) \quad (6)$$

where the first term in parentheses is the correction factor for back radiation in the absence of clouds, e_a is the vapour pressure of water at a standard height, and the second term in parentheses is the correction for cloud effects based on cloud cover (n_c) measured at the Skaftafell meteorological station on the days of the aerial survey.

For sensible heat flux, equation (4) is used, and the input values were taken from a combination of literature and meteorological station data. Latent heat flux (equation (5)) requires that the saturated specific humidity at the surface (q^*_s) is calculated from the saturated vapour pressure (e^*_s) at the surface. The same relationship was then used to calculate the specific humidity of the air (q_a) from the vapour pressure of the air (e_a).

$$q^*_s = \frac{\lambda e^*_s}{P_o + (\lambda - 1) e^*_s} \quad (7a)$$

$$q_a = \frac{\lambda e_a}{P_o + (\lambda - 1) e_a} \quad (7b)$$

where λ ($=0.622$) is the ratio of gas constants for dry and moist air (Garratt 1992) and P_o is the air pressure in hPa (from meteorological station at Grímsvötn).

The saturated vapour pressure of the surface was calculated using equation (8a), followed by the saturated vapour pressure of the air from a similar relationship (8b). Once a correction for the known relative humidity is included, the vapour pressure

of the air can be calculated from equation (9).

$$e_{*s} = 6.112 \exp \left[\frac{[17.67(T_s - 273.15)]}{(T_s - 29.65)} \right] \quad (8a)$$

$$e_{*a} = 6.112 \exp \left[\frac{[17.67(T_a - 273.15)]}{(T_a - 29.65)} \right] \quad (8b)$$

$$e_a = \text{Relative Humidity} \times e_{*a} \quad (9)$$

Equations (8a) and (8b) are identical except for substituting the air temperature for the surface temperature. In this study, data from six nearby meteorological stations (Skaftafell, Hjarðarnes, Höfn, Akurnes, Vagnsstaðir, Kirkjubæjar-klaustur) were collected, but relative humidity readings were only available from two of those for June 2001. Therefore, relative humidity was taken as an average of the two. When the results from equations (7) to (9) are inserted into equations (5) and (6), a value for the latent heat flux and upward longwave radiation can be determined.

The final parameter needed for the total upward heat flux is the incoming shortwave solar radiation. As this was not collected at the time of the survey, a value has been taken from the literature. In 2001, Gudmundsson *et al.* (2003) derived a number of models for summer ablation on Langjökull ice sheet, Iceland, using climatic data necessary for heat flux calculation. Their measure for incoming shortwave solar radiation was 280 W m^{-2} , which has been used for this research. An average constant for the proportion of solar radiation reflected over lakes has been taken as 7% from Oke (1995) to obtain a downward flux of 260 W m^{-2} .

3.2 Geomorphological mapping

Of the aerial photographs collected during the 2001 survey, 12 colour prints, taken from the central flight line, show the entire Grímsfjall ridge, and these were chosen for analysis. The photographs were scanned, as both digital and hardcopy photographs were needed for use in digitizing and stereoscopy, with a resolution of 300 dpi. They were then co-registered to a geometrically corrected ATM image, within ERDAS imagine (ERDAS 1999). A high-resolution mirror stereoscope was used to analyse the original hard copy photographs, and key features were outlined and digitized onscreen within ArcMap.

4. Results

4.1 Heat flux

Surface observations of the crater lake on 3 and 9 June 2001 accord well with the results from the thermal imagery (figures 2 and 3). Although water temperature measurements could not be made, figure 4(a) shows that the crater lake is ice free with steam rising from water by the south shore, where the thermal image for 10 June (figure 2) indicates temperatures of $40\text{--}45^\circ\text{C}$. Figure 4(b) shows the larger, exposed part of the caldera lake to the west of the 1998 eruption site. This lake is partly covered by floating ice although the extreme eastern end (seen in foreground on figure 4(a)) was completely ice free with steam rising from the water by the southern shore, as in the smaller crater lake. The thermal image (figure 2) shows that



(a)



(b)

Figure 4. (a) The crater lake in Grímsvötn on 3 June 2001. Note the steam rising from the southern (right-hand) margin of the lake, indicating high temperatures in agreement with the thermal imagery (figure 2). (b) The western part of the exposed caldera lake. Most of the lake was covered by thin floating ice.

the partly ice-covered lake has temperatures close to zero with the exception of the extreme eastern end, where temperatures of 40–45°C occur by the southern shore.

Using data from 10 June 2001 and the parameters listed in table 1 and equation (2), the total upward flux from the crater lake can be calculated:

$$Q_T = Q_{Lo} + Q_{Sh} + Q_{LE} - Q_{Si} = 108 + 298 + 794 - 260 = 940 \text{ W m}^{-2}$$

For the lake area of 10 600 m², this equates to a total energy of 10 MW. This heat flux is about an order of magnitude higher than the 50–100 W m⁻² average found for the Grímsvötn calderas (Björnsson and Gudmundsson 1993), confirming that patches of open water along the caldera faults are signs of ‘hot spots’, or places of intense geothermal activity.

The above result is based on a mean temperature for all the pixels across the lake surface. However, it is possible to calculate the heat flux for each individual 5 × 5 m

Table 1. Parameters used in the calculation of heat flux from Grímsvötn 1998 crater lake.

Parameter		Value
ϵ_s	Emissivity of water	0.985
σ	Stefan–Boltzmann constant	$5.67 \times 10^{-8} \text{ W m}^{-2} \text{ K}^{-4}$
ρ	Air density	1 kg m^{-3}
C_p	Specific heat capacity of air	$1005 \text{ J kg}^{-1} \text{ K}^{-1}$
C_e	Transfer coefficients for sensible and latent heat	1.4×10^{-3}
U_a	Wind speed	6.8 m s^{-1}
T_s	Lake surface temperature	305 K
T_a	Mean air temperature	274.15 K
L	Latent heat of evaporation	$2.5 \times 10^6 \text{ J kg}^{-1}$
q_s^*	Saturated specific humidity at water surface	0.0374
q_a	Specific humidity at reference height (10 m above lake)	0.0039
e_s^*	Saturated vapour pressures at the surface	48.38
e_a	Vapour pressure of the air	5.19

pixel. Figure 5 is a histogram of the heat flux across the lake derived from calculating the heat flux for every pixel in the lake. It shows that, based on a constant set of values for wind speed, air temperature and relative humidity, there is some variability over the lake for the two dates surveyed. The histogram for 14 June shows a near normal distribution, but the 10 June histogram shows greater variability, with higher heat flux values being evenly distributed. The overall heat flux is higher on 14 June 2001, with a mean value of 1100 W m^{-2} compared to 1040 W m^{-2} for 10 June. This difference is, however, not significant considering that there are uncertainties in air temperature, wind speed and humidity for both dates.

This calculation of heat flux was based on wind speeds of 6.8 m s^{-1} (10 June 2001) and 6.7 m s^{-1} (14 June 2001), which were the average wind speeds taken from the Skaftafell meteorological station. These are likely to be lower than the windspeeds at Grímsvötn and the calculated heat flux will therefore be a minimum. When a sensitivity analysis was undertaken, wind speed was found to be the most influential factor. To reduce uncertainty during further surveys of this type, it is important to

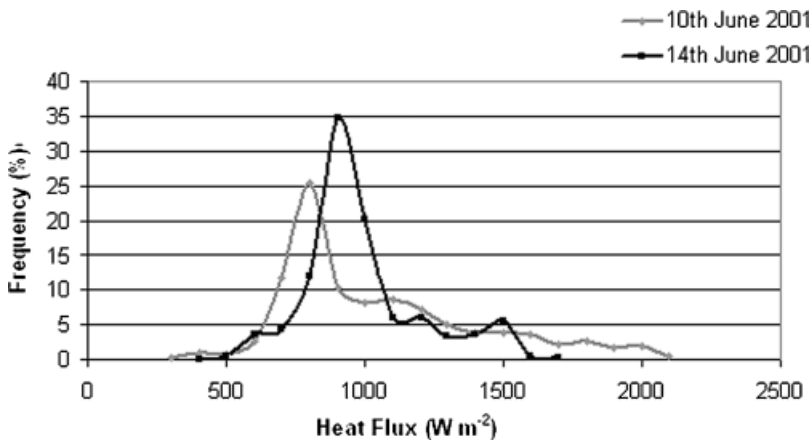


Figure 5. Histogram distribution for heat flux, pixel by pixel across the 1998 crater lake, for 10 and 14 June 2001.

collect accurate wind speed data on an ice sheet such as Vatnajökull, where wind speeds and weather can be extreme and change rapidly.

To obtain an idea of the total heat output from open water to the atmosphere, the size and average surface water temperatures for the other three localities with open water (northeast cauldron, east caldera lake and west caldera lake; see figure 2) were estimated using the thermal images. The results for all four patches of open water are given in table 2. The coldest spots (cauldron and west caldera lake) are in fact gaining energy whereas the two hotter areas combined are losing about 20 MW. The net heat exchange is estimated as 18 MW. There are considerable uncertainties in this value but it can conservatively be regarded as a robust order of magnitude estimate. With the exception of the crater lake, all these spots are partly or fully ice-bounded and partly covered by floating ice. Water temperatures above freezing will therefore cause ice melting. Thus, the heat flux from the underlying geothermal areas into the ice-bounded lakes is expected to be much greater than implied by the values in table 2. This is supported by a study (Jarosch and Gudmundsson 2007) of enhanced ice melting between 1999 and 2004 along the easternmost part of the Grímsfjall ridge that led to the formation of a 1.4-km-long line of large depressions including the northeast cauldron. Jarosch and Gudmundsson's (2007) ice flow modelling indicates geothermal heat flux values of a few hundred W m^{-2} and an average heat output of 250–300 MW. This demonstrates that, although an ice-bounded lake within a glacier is not losing significant heat to the atmosphere, its existence implies highly elevated heat flux.

4.2 Geomorphological map

The 1998 eruption site (figure 6, C3) is a complex region containing a large number of different geomorphological units. Sviahnkur vestri is a high peak to the southeast of the eruption site. Numerous debris fans and slumps cover the cliff along this section of the Grímsfjall ridge (figure 6, C4). Circulation of water through the poorly consolidated debris piles leads to more instabilities in the region (Gudmundsson 1989). The large area of tephra in the 1998 crater appears to be undifferentiated in the aerial photographs and was mapped as one unit. The caldera lake is in two distinct sections. The west caldera lake is mostly ice and firn covered (figure 6, B3), apart from the small water section on the eastern edge, where it is in contact with the tephra. The east caldera lake (figure 6, C2) is also mostly firn covered with occasional icebergs. The exposed water with a mean temperature of 289 K (table 2) forms a thin sliver along the edge of the tephra. This is probably due to the water being cycled through the tephra pile and emitted through steam vents, giving the tephra an apparent residual heat, allowing the edges of the caldera lake to remain

Table 2. Heat output from open water in June 2001.

	Area m^2	T_s K	Q_{Lo} W m^{-2}	Q_{sh_2} W m^{-2}	Q_{Le} W m^{-2}	Q_{Si} W m^{-2}	Q_{T} W m^{-2}	P MW
Cauldron northeast	30000	277	74	28	50	180*	-28	-1
Caldera lake east	50000	289	88	142	225	260	195	10
Crater lake	10600	305	108	298	794	260	940	10
Caldera lake west	20000	275	72	88	31	260	-69	-1
Total								18

*About 30% of the lake in the cauldron was in shadow, leading to lower shortwave radiation.

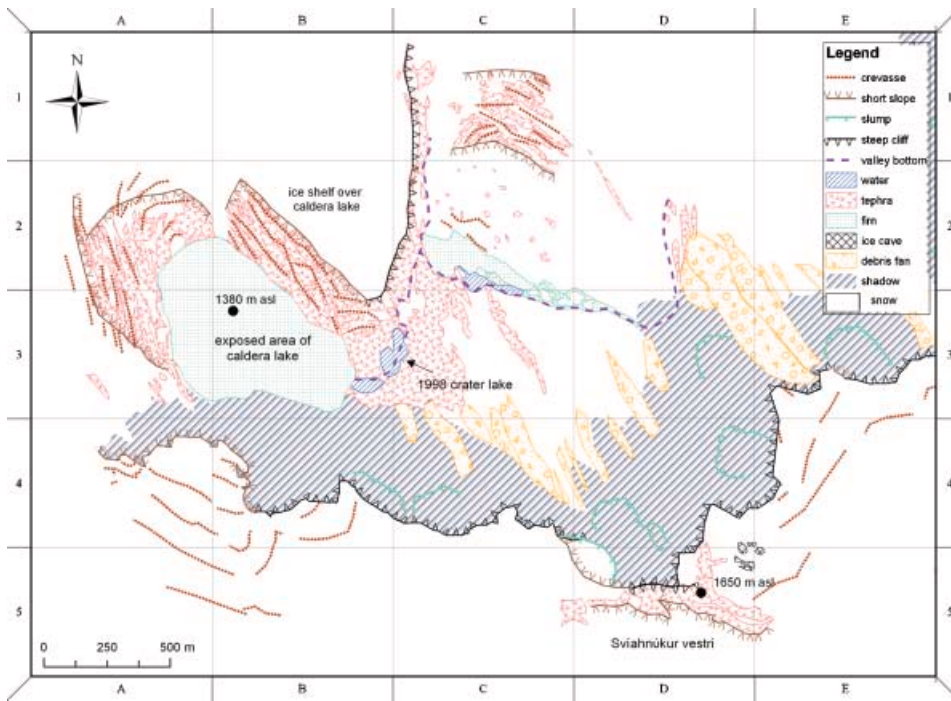


Figure 6. Geomorphological map of the 1998 eruption site. The map also shows an exposed section of the caldera lake and Grímsfjall ridge.

liquid. The 1998 crater lake (at the junction of B3 and C3) within the tephra itself is visible along the valley bottom of the eruption site.

5. Discussion

This study has shown that it is possible to calculate heat flux values from lake surface to atmosphere in a glacial setting using water surface temperatures and meteorological data. However, further study is required to quantify the errors in heat flux calculations, because critical measurements, such as wind speed were not made locally at the time of the survey. Consequently, it is essential during future surveys over water bodies that accurate ground measurements of wind speed are collected at the time of aerial surveys.

The thermal imagery provided an insight into the heat output along Grímsfjall, revealing elevated temperature regions that were not detected during ground-based surveys. These include thermal anomalies that follow the trend of the caldera fault (Gudmundsson 1989), along the southern wall of the caldera (figure 2). A total heat loss to the atmosphere of ~ 18 MW is estimated during the survey period. The total thermal power of Grímsvötn has not been estimated in detail for this period but ice melting along the southern caldera fault in 2000–2001 (Institute of Earth Sciences, University of Iceland, unpublished data) suggests that the thermal power was above the long-term base value of 1500–2000 MW (Björnsson and Gudmundsson 1993). Thus, in 2001 when the combined area of open water was about 0.1 km^2 (figure 2 and table 2), heat loss to the atmosphere was two orders of magnitude less than the total heat output from geothermal activity. This shows that ice melting was the

dominant style of heat release. Considerably larger open water patches are required for the heat loss to become an important component in the overall heat budget of Grímsvötn.

Several studies have shown that meltwater temperatures above the pressure melting point of ice substantially increase the development of englacial and subglacial tunnels (e.g. Clarke 1983, Björnsson 1992). Events during the Gjalp eruption in Vatnajökull in 1996 demonstrated this effect, when meltwater, at a temperature of about 20°C, was released from the eruption site (Gudmundsson *et al.* 1997). In the present study, the airborne imagery showed that the meltwater lakes along the Grímsfjall ridge have an average temperature exceeding 20°C mid-way between two eruptions. The existence of such warm water in parts of the lake may be a contributing factor, together with increased geothermal activity under the ice dam east of the lake (Institute of Earth Sciences, unpublished data), in keeping subglacial waterways open and sustaining the pervasive leakage of water from Grímsvötn over the past several years.

The two thermal images collected 4 days apart have shown that there are small apparent temperature differences on this time-scale. The possible reasons for these include factors not fully accounted for in the preprocessing of the two images, such as variations in reflected solar radiation, atmospheric attenuation and image acquisition differences, or real changes in land surface thermal characteristics caused by episodic events such as cornice collapses from along the Grímsfjall ridge. Such factors will have to be taken into account during any future surveys by ensuring that there are adequate ground observations, good onboard Global Positioning System (GPS)/positional data acquisition, day and night imagery, and atmospheric measurements at the time of the flight.

This study has demonstrated the usefulness of two different techniques, using aerial imagery, applied to an active subglacial volcano. The geothermal activity of Grímsvötn is the source of the instabilities along the Grímsfjall ridge, along with the geomorphological features, such as crevasses and ice caves, in the region around Grímsvötn. Geothermal activity leads to water cycling through tephra and rock, leading to instabilities of the cornices on top, and slumps along the side of the Grímsfjall ridge. Hence, the measurements of heat flux for different areas of open water around the caldera can be combined with the geomorphological map to establish regions of the caldera that should be monitored. In conclusion, this study has demonstrated the potential contribution of remotely sensed data (together with the requisite ground-based data) to developing a deeper understanding of the complex and inter-related volcanic, glacial and geomorphological processes that are associated with subglacial volcanoes.

Acknowledgements

We thank the Natural Environmental Research Council (NERC) Airborne Research and Survey Facility (ARSF) for collecting the data in 2001. We also thank Andrew Wilson and Bill Mockridge for their assistance in the geocorrection of the imagery, Ian Jones for his assistance and discussions of heat flux, and Matt Ball for his assistance in temperature conversion of the ATM imagery.

References

- BJÖRNSSON, H., 1983, A natural calorimeter at Grímsvötn; an indicator of geothermal and volcanic activity. *Jökull*, **33**, pp. 13–18.

- BJÖRNSSON, H., 1988, Hydrology of ice caps in volcanic regions. *Societas Scientiarum Islandica*, **45**, pp. 1–139.
- BJÖRNSSON, H., 1992, Jökulhlaups in Iceland: prediction, characteristics and simulation. *Annals of Glaciology*, **16**, pp. 95–106.
- BJÖRNSSON, H., 2003, Subglacial lakes and jökulhlaups in Iceland. *Global and Planetary Change*, **35**, pp. 255–271.
- BJÖRNSSON, H., 2004, Glacial lake outburst floods in mountain environments. In *Mountain Geomorphology*, P.N. Owens and O. Slaymaker (Eds), pp. 165–184 (London: Arnold).
- BJÖRNSSON, H. and GUDMUNDSSON, M.T., 1993, Variations in the thermal output of the subglacial Grímsvötn caldera, Iceland. *Geophysical Research Letters*, **19**, pp. 2127–2130.
- CLARKE, G.K.C., 1983, Glacier outburst flood from ‘Hazard Lake’, Yukon Territory, and the problem of flood magnitude prediction. *Journal of Glaciology*, **28**, pp. 3–21.
- EINARSSON, P., BRANDSDOTTIR, B., GUDMUNDSSON, M.T., BJÖRNSSON, H., GRÖNVOLD, K. and SIGMUNDSSON, F., 1997, Center of the Iceland hotspot experiences volcanic unrest. *EOS, Transactions, American Geophysical Union*, **78**, pp. 374–375.
- ERDAS 1999, *ERDAS Imagine Field Guide* (Atlanta: ERDAS Inc.).
- GARRATT, J.R., 1992, *The Atmospheric Boundary Layer*, Cambridge Atmospheric and Space Science Series (Cambridge: Cambridge University Press).
- GILL, A.E., 1982, *Atmosphere–Ocean Dynamics*. International Geophysics Series, vol. 30 (London: Academic Press).
- GUDMUNDSSON, M.T., 1989, The Grímsvötn caldera, Vatnajökull: subglacial topography and structure of caldera infill. *Jökull*, **39**, pp. 1–9.
- GUDMUNDSSON, M.T., 2003, Melting of ice by magma–ice–water interactions during subglacial eruptions as an indicator of heat transfer in subaqueous eruptions. *Geophysical Monograph*, **140**, pp. 61–72.
- GUDMUNDSSON, M.T., SIGMUNDSSON, F. and BJÖRNSSON, H., 1997, Ice–volcano interaction of the 1996 Gjálp subglacial eruption, Vatnajökull, Iceland. *Nature*, **389**, pp. 954–957.
- GUDMUNDSSON, M.T., SIGMUNDSSON, F., BJÖRNSSON, H. and HÖGNADOTTIR, T., 2004, The 1996 eruption at Gjálp, Vatnajökull ice cap, Iceland: efficiency of heat transfer, ice deformation and subglacial water pressure. *Bulletin of Volcanology*, **66**, pp. 46–65.
- GUDMUNDSSON, S., BJÖRNSSON, H. and PALSSON, F., 1995, Changes in jökulhlaup sizes in Grímsvötn, Vatnajökull, Iceland, 1934–91, deduced from in-situ measurements of subglacial lake volume. *Journal of Glaciology*, **41**, pp. 263–272.
- GUDMUNDSSON, S., BJÖRNSSON, H., PALSSON, F. and HARALDSSON, H.H., 2003, Physical energy balance and degree-day models of summer ablation on Langjökull ice cap, SW Iceland. *Raunvisdastofnun Haskolans*, RH-20-2003.
- HICKS, B.B., 1972, Some evaluations of drag and bulk transfer coefficients over water bodies of different sizes. *Boundary Layer Meteorology*, **3**, pp. 201–213.
- JAROSCH, A.H. and GUDMUNDSSON, M.T., 2007, Numerical studies of ice flow over subglacial geothermal heat sources at Grímsvötn, Iceland, using the full Stokes equations. *Journal of Geophysical Research*, **112**, pp. F02008, doi:10.1029/2006JF000540.
- JONES, I., GEORGE, G. and REYNOLDS, C., 2005, Quantifying effects of phytoplankton on the heat budgets of two large limnetic enclosures. *Freshwater Biology*, **50**, pp. 1239–1247.
- OKE, T.R., 1995, *Boundary Layer Climates*, 2nd edn (London: Routledge).
- SIGMUNDSSON, F. and GUDMUNDSSON, M.T., 2004, The Grímsvötn eruption, November 2004. *Jökull*, **54**, pp. 139–142.
- SMELLIE, J.L., 1999, Subglacial eruptions. In *Encyclopedia of Volcanoes*, H. Sigurdsson (Ed.), pp. 403–418 (San Diego: Academic Press).
- STEWART, S.F., PINKERTON, H., BLACKBURN, G.A. and GUDMUNDSSON, M.T., 2007, Comparison and validation of Airborne Thematic Mapper thermal imagery with ground-based temperature data for Grímsvötn caldera, Vatnajökull, Iceland. *Geological Society, London, Special Publications*, **283**, pp. 31–43.

- THORDARSON, T. and LARSEN, G., 2007, Volcanism in Iceland in historical time: volcano types, eruption styles and eruptive history. *Journal of Geodynamics*, **43**, pp. 118–152.
- VOGFJÖRD, K.S., JAKOBSDOTTIR, S.S., GUDMUNDSSON, G.B., ROBERTS, M.J., ÁGUSTSSON K., ARASON, T., GEIRSSON, H., KARLSDOTTIR, S., HJALTADOTTIR, S., OLAFSDOTTIR, U., THORBJARNARDOTTIR, B., SKAFTADOTTIR, T., STURKELL, E., JONASDOTTIR, E.B., HAFSTEINSSON, G., SVEINBJORNSSON, H., STEFANSSON, R. and JONSSON, T.V., 2005, Forecasting and monitoring a subglacial eruption in Iceland. *EOS, Transactions, American Geophysical Union*, **26**, pp. 246–247.